Experimental study of laser-induced isomerization dynamics of specific C_{2}H_{2}^{q} ions

Bethany Jochim, M. Zohrabi, T. Severt, Ben Berry, K. J. Betsch, Peyman Feizollah, Jyoti Rajput, E. Wells, K. D. Carnes, and I. Ben-Itzhak

Experimental study of laser-induced isomerization dynamics of specific C$_2$H$_2^q$ ions

Bethany Jochim,[1] M. Zohrabi,[1] T. Severt,[1] Ben Berry,[1] K. J. Betsch,[1] Peyman Feizollah,[1] Jyoti Rajput,[1] E. Wells,[2] K. D. Carnes,[1] and I. Ben-Itzhak[1]

[1]*J. R. Macdonald Laboratory, Department of Physics,*
Kansas State University, Manhattan, Kansas 66506 USA
[2]*Department of Physics, Augustana University, Sioux Falls, South Dakota 57197 USA*
(Dated: December 4, 2019)

We investigate intense, ultrafast laser-induced isomerization and two-body fragmentation of acetylene monocations and dications using coincidence three-dimensional momentum imaging. Whereas the vast majority of previous work on strong-field isomerization and fragmentation of acetylene has necessarily involved ionization, by focusing solely on dissociation of ion-beam targets, we ensure that the dynamics ensue within a single molecular ion species, potentially simplifying interpretation. We demonstrate the rich information that can be extracted from such a measurement and discuss advantages and disadvantages of this approach.

I. INTRODUCTION

Measuring the photo-induced breakup of hydrocarbons has been demonstrated as a valuable means of examining isomerization reactions, specifically hydrogen migration. Numerous light sources have been used for these studies [1], which are most commonly performed by irradiating neutral target molecules to initiate dynamics.

One specific molecule that has attracted a great deal of interest as a prototype for studying isomerization is acetylene, which has the linear HCCH configuration in its ground state. Isomerization of this molecule entails migration of a hydrogen from one carbon site to the other to form the vinylidene isomer, H$_2$CC. Key investigations into the photofragmentation of C$_2$H$_2$ [2–17] have taken advantage of powerful coincidence three-dimensional (3D) momentum imaging techniques, such as cold target recoil ion momentum spectroscopy (COLTRIMS) [18, 19]. In these studies, one commonly-used signature of C$_2$H$_2$ isomerization has been measurement of the C$^+$ + CH$_2^+$ channel for rearrangement into the vinylidene configuration. Measurement of CH$^+$ + CH$^+$, in contrast, has been taken as a signature for remaining in the acetylene configuration.

Other means of identifying C$_2$H$_2$ isomerization include monitoring the molecule's structural changes through the relative angles of the fragment momenta in three- and four-body Coulomb explosion imaging (CEI) measurements [4, 5, 7, 11, 14], which involve triple or quadruple ionization, respectively. While CEI has its own limitations [16, 20, 21], the fact that ionization is involved by necessity in the observation of all these signatures and that the final charge state is not necessarily the same as that undergoing isomerization may also obscure interpretation. Based on these types of signatures, some studies have concluded that C$_2$H$_2$ isomerization occurs in the monocation [12, 22–24], while others have pointed to the dication states [2–4, 6, 8–17, 25]. It is important to note that these different interpretations are not necessarily conflicting, as the particular pathways could depend sensitively upon the experimental parameters. However,

they may also indicate some ambiguity in the interpretation.

The rich information provided by the aforementioned coincidence momentum imaging techniques, such as the kinetic energy release (KER) and angular distributions, can be illuminating in determining which potential energy surfaces may be involved in the isomerization and pathways toward the final products [6, 8]. The dynamics, however, can be quite complex. For molecules exposed to intense laser fields, it is probable that many multiphoton pathways contribute to the measured data, making interpretation challenging. As a specific example, for dissociative double ionization of C$_2$H$_2$ by an intense 800-nm femtosecond laser pulse, the common interpretation that hydrogen migration occurs exclusively in the dication [4, 13–15, 17, 24, 26] awaits more direct substantiation. Here, the signature dissociative ionization channels likely involve the exchange of many photons with the laser field. Thus, despite the detailed information provided by the measurements, one cannot readily exclude the case in which hydrogen migration is initiated or completed in the neutral or monocation intermediate states before the final ionization step(s). Hence, as pointed out by Gong *et al.* [12], experimental determination of the charge state in which isomerization occurs is a highly-coveted goal.

While Gong and co-workers [12] used above-threshold double ionization of acetylene to distinguish hydrogen migration on the monocation and dication surfaces of C$_2$H$_2$, in this article we propose a complementary approach that restricts isomerization to a specific C$_2$H$_2^q$ molecular ion. In this approach, we perform kinematically-complete measurements of laser-induced dissociation of molecular ions, introduced as a beam target, sidestepping altogether the ambiguity introduced by ionization. Here, the laser field excites the molecule to a dissociative state of the same charge and may also initiate isomerization. Thus, laser intensities lower than that required for ionization may be used, limiting the contributions of complex multiphoton pathways and reducing the number of potential surfaces involved. While the dilute nature of

an ion-beam target leads to lower counting rates than can be achieved with gas-phase targets, none of the detailed information provided by other coincidence 3D momentum imaging techniques is sacrificed. Note that the focus of this manuscript is mainly to present this approach, which can be quite powerful in making future advances in studying isomerization of $C_2H_2^q$ and other molecular ions. At present, however, further work is needed to attain deeper understanding of the dynamics.

II. EXPERIMENTAL METHOD

We demonstrate this method for studying $C_2H_2^q$ isomerization limited to a particular charge state using $C_2D_2^{2+}$ and $C_2H_2^+$ as specific examples. Our experiment is illustrated in Fig. 1. Molecular ions are produced via fast electron impact in an electron-cyclotron resonance (ECR) ion source. The $C_2D_2^{2+}$ and $C_2H_2^+$ beams are generated by loading this ion source with CD_4 and C_2H_2 gas, respectively. The ions are accelerated upon extraction from the ECR source to energies of 42 keV and 8 keV for the $C_2D_2^{2+}$ and $C_2H_2^+$ beams, respectively. The ion beam is selected by a magnet and then electrostatically steered and focused to produce a collimated target that has a $\sim 0.9 \times 0.9$ mm^2 cross section at its intersection with the laser beam. The flight time of the target molecular ions from the ion source to the intersection with the laser is ~ 10 μs for $C_2D_2^{2+}$ and ~ 20 μs for $C_2H_2^+$.

Based on electron impact ionization studies, the $C_2H_2^+$ target is known to be predominantly in the acetylene (linear HCCH) configuration [27–30]. While the production mechanism for the dication beam from methane gas is admittedly less straightforward than that of the $C_2H_2^+$ beam, the $C_2D_2^{2+}$ beam is also most likely in the acetylene configuration [31].

The initial state of molecular ions at the moment they are probed by a laser pulse is a consequence of their production via fast electron impact in the ion source and the ensuing decay processes occurring during their flight to the laser interaction region. While fast electron impact preferentially populates lower electronic states, highly-excited states may also be populated. Moreover, this ionization is a vertical transition involving minimal angular momentum transfer. Therefore, the rotational population is similar to that of neutral molecules at room temperature [32, 33], and the Franck-Condon principle provides a good estimate of the vibrational population [32–34]. The long flight time to the interaction region (tens of microseconds) allows decay of the excited electronic states, as in most cases radiative decay proceeds much faster than the flight times. The exception to this trend is the case of metastable electronic states, e.g., those requiring a spin flip for decay to the electronic ground state [35, 36]. For the $C_2H_2^+$ beam, a metastable state may be initially populated [37], as discussed in Sec. III B, but more complete structure and lifetime information is essential to say with certainty that this is the case. We note
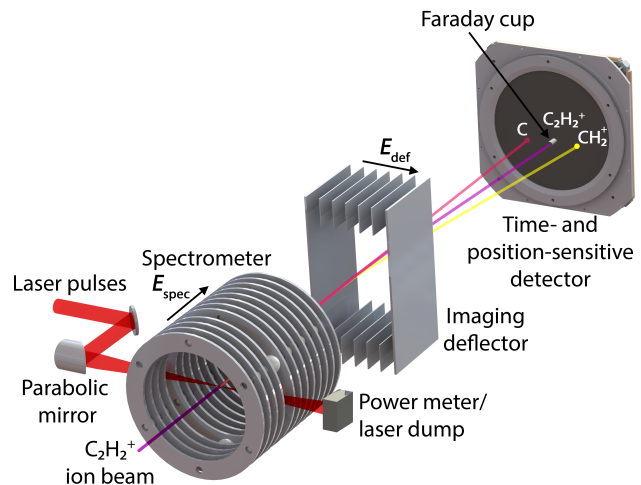
FIG. 1. Schematic of the coincidence 3D momentum imaging setup, illustrated with the $C_2H_2^+ \rightarrow C + CH_2^+$ breakup channel. A laser beam of femtosecond pulses intersects the ion beam inside the spectrometer. The laser-induced fragments are separated in time by a longitudinal field E_{spec}, created by the spectrometer. The fragments are also separated in position by E_{def}, a transverse field created by an imaging deflector.

that the present $C_2D_2^{2+}$ target is likely vibrationally and rotationally hot due to its formation from methane via "source chemistry," [31] but this molecule is still most likely in the electronic ground state when probed by the laser.

The Ti:Sapphire laser system used in this study creates Fourier-transform-limited (FTL) pulses of ~ 790-nm central wavelength, ~ 60-nm bandwidth [full width at half maximum (FWHM)], 2-mJ energy, and ~ 23-fs duration (FWHM in intensity) [38]. The pulse duration is measured using second harmonic generation frequency-resolved optical gating (SHG-FROG) [39]. An $f = 203$-mm focal length 90° off-axis parabolic mirror focuses the laser beam onto the ion-beam target. Translation of the laser focus away from the ion-beam center and/or insertion of power-attenuating optics enable control of the peak intensity of the laser [35, 40]. We also utilize second harmonic pulses, which are produced by sum frequency generation in a β-barium borate (BBO) crystal [41]. The measured spectrum centroid for these pulses is ~ 395 nm with a bandwidth of ~ 10 nm (FWHM). Their temporal duration, measured by self diffraction frequency resolved optical gating (SD-FROG) [42], is ~ 50 fs (positively chirped). The FTL limit for the second-harmonic pulses is about 23 fs.

The laser-induced fragments are measured in coincidence using a position- and time-sensitive detector downstream, allowing evaluation of their complete 3D momenta. From the momenta, the KER and angular distributions are retrieved. Importantly, the keV energy of the ion beam allows us to also measure the neutral fragments. Therefore, we can perform kinematically-complete measurements of the dissociation channels of

keV beams, such as $C_2H_2^+ + n\omega \to C^+ + CH_2$. Additional details about this experimental method can be found in Refs. [43–47].

Similar to several of the studies mentioned in the introduction, we use $C_2H_2^q \to C^{q_1} + CH_2^{q_2}$ ($q = q_1 + q_2$) measurement as a signature of isomerization from the acetylene configuration to the vinylidene configuration. We note here that this does not preclude the possibility of isomerization of C_2H_2 ions that remain bound. While we can detect these molecular ions through use of an imaging deflector, we cannot determine their internal configuration.

III. RESULTS AND DISCUSSION

A. $C_2D_2^{2+}$

In the $C_2D_2^{2+}$ case, as expected, acetylene-like breakup, $CD^+ + CD^+$ (A), and vinylidene-like breakup, $C^+ + CD_2$ (V), are observed, as shown by the coincidence time-of-flight (CTOF) spectrum in Fig. 2. Imposing momentum conservation on these identified channels, we obtain their branching ratios. At 798-nm central wavelength and peak intensity 5×10^{15} W/cm^2, the acetylene branching ratio is $A/(A + V) \sim 51.5 \pm 3.5\%$. In contrast, the acetylene branching ratio measured with 392-nm pulses at peak intensity 6×10^{14} W/cm^2 is $\sim82.9 \pm 2.1\%$, a significant difference. This observation points to the possibility of controlling $C_2D_2^{2+}$ isomerization with laser parameters like wavelength, pulse duration, and intensity. While control of isomerization [13, 26, 48–50] and fragmentation [10, 49, 51–55] have been topics of significant exploration, their study utilizing a molecular-ion-beam approach would enable focusing on dissociation, in contrast to the previous studies that examined dissociative ionization.
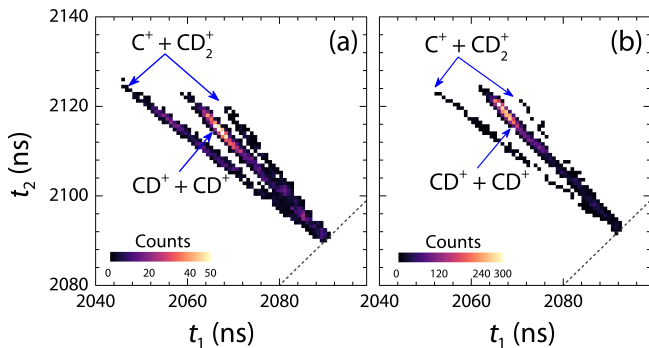
FIG. 2. The coincidence time-of-flight (CTOF) spectra of the dissociation channels $CD^+ + CD^+$ (A) and $C^+ + CD_2^+$ (V) for (a) 798-nm pulses and (b) 392-nm pulses after imposing momentum conservation. The gray dashed line indicates where $t_1 = t_2$. Under the present experimental conditions, in the V channel, CD_2^+ fragments may sometimes reach the detector before C^+ fragments. This is manifested by the righthand branch of the V channel.
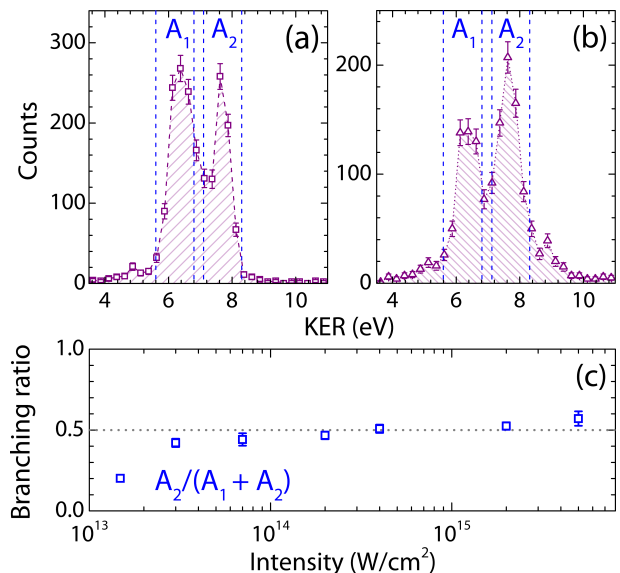
FIG. 3. Kinetic energy release (KER) spectra for the $CD^+ + CD^+$ channel measured at 798-nm wavelength and peak intensity (a) 5×10^{13} W/cm^2 and (b) 5×10^{15} W/cm^2. (c) Branching ratio of KER peaks A_1 and A_2 as a function of peak intensity. The regions marked by the blue dashed lines in panels (a) and (b) indicate where the yields of these peaks were evaluated.

The KER spectra for the A channel measured with 798-nm photons are shown in Fig. 3(a) and (b). This channel exhibits two peaks centered at ~6.3 eV (A_1) and ~7.6 eV (A_2). The fact that A_1 and A_2 are separated by close to the energy of one photon could indicate that they are due to pathways involving the absorption of n and $n + 1$ photons, respectively, and have the same dissociation limit. The contribution of the higher-KER peak, A_2, grows with respect to A_1 as the laser intensity increases, shown by the branching ratio in Fig. 3(c). This enhancement of peak A_2 is consistent with the suggestion that its underlying process is an $n + 1$–photon process (i.e., above-threshold dissociation), in contrast to an n–photon process associated with A_1. However, future work is needed for deeper understanding of the underlying pathways, as well as the observed competition between the two KER peaks.

Curiously, the KER peaks A_1 and A_2 are markedly different from the ~5-eV KER measured for the $CH^+ + CH^+$ (A) channel in studies of neutral C_2H_2 targets. These neutral-target studies involved probing C_2H_2 with laser pulses similar to ours [3] or removing a carbon k-shell electron, leading to double ionization [6].

To shed light on this dissimilarity, we explore possible dissociation pathways leading to the measured $CD^+ + CD^+$ ($CH^+ + CH^+$) products, assuming that the target is in the acetylene configuration when probed by the laser, as stated in Sec. II. We utilize potential energy curves corresponding to the C–C stretch of the linear acetylene dication, reported by Thissen et al. [56].
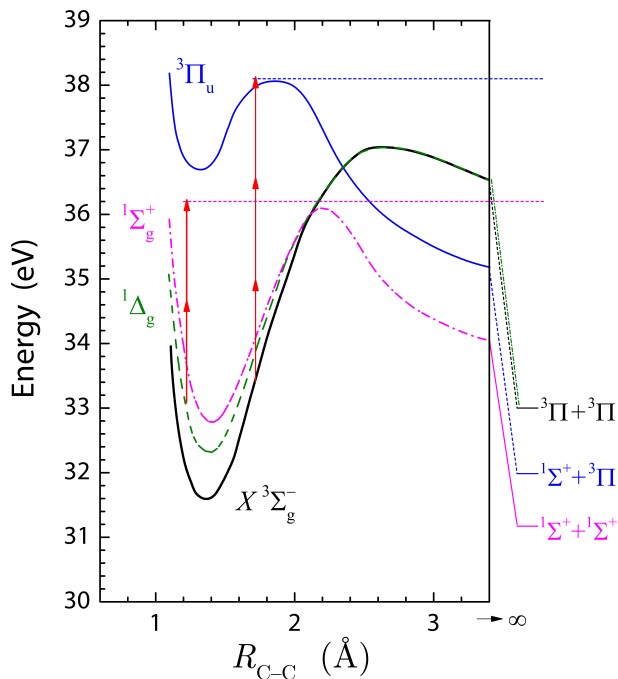
FIG. 4. A few of the lowest potential energy curves for the C–C stretch of the linear HCCH dication (with the C–H bond fixed at its equilibrium distance). Adapted from Ref. [56].

These potentials are shown in Fig. 4. For the neutral-target studies mentioned above [3, 6], it seems reasonable that the 5-eV measured KER is associated with over-the-barrier dissociation involving the $^1\Sigma_g^+$ state. This state has a barrier along the C–C stretch coordinate leading to the lowest $CH^+ + CH^+$ limit ($^1\Sigma^+ + {}^1\Sigma^+$, labeled in Fig. 4). The barrier lies about 5 eV above this dissociation limit. In the strong-field case [3], the vibrational continuum of the $^1\Sigma_g^+$ state can be reached by multiphoton ionization. Alternatively, multiphoton ionization can lead to population of the lowest singlet electronic state of the dication, $^1\Delta_g$. Following that, two-photon excitation to the $^1\Sigma_g^+$ state, indicated by the arrows in Fig. 4, may lead to over-the-barrier dissociation, similar to when the $^1\Sigma_g^+$ state is populated directly. The triplet electronic states of the linear acetylene dication, on the other hand, lead to KER that is lower (barrier of $X\,^3\Sigma_g^-$ is ~4 eV above $^3\Pi + {}^3\Pi$) or higher (barrier of $^3\Pi_u$ is ~6 eV above $^1\Sigma^+ + {}^3\Pi$) than that of the pathways involving the singlets and therefore are not the main contributors in the case of photofragmentation starting from neutral C_2H_2 targets.

In contrast, the triplet states play a dominant role in the present case, as $C_2D_2^{2+}$ ions arrive to the interaction region in the $X\,^3\Sigma_g^-$ electronic ground state, as explained in Sec. II. Because the laser field does not couple states of different spin multiplets, the dissociation pathways dominating the previous neutral C_2H_2 studies [3, 6] are closed, assuming that there are no metastable states initially populated. Instead, the dication may dissociate
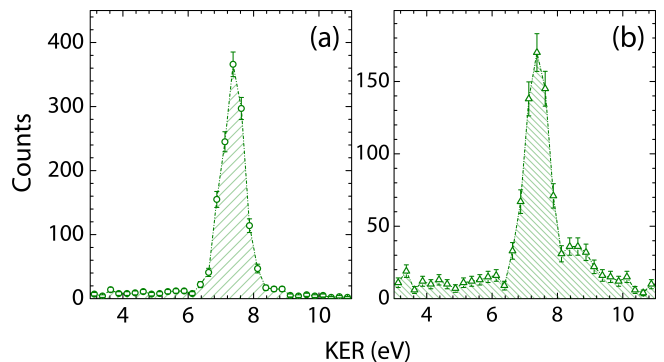
FIG. 5. Kinetic energy release (KER) spectra for the $C^+ + CD_2^+$ channel measured at 798-nm wavelength and peak intensity (a) 5×10^{13} W/cm^2 and (b) 5×10^{15} W/cm^2.

by three-photon absorption to the $^3\Pi_u$ state, as shown in Fig. 4. The $^3\Pi_u$ state barrier along the C–C stretch coordinate lies about 6 eV above its associated dissociation limit, $^1\Sigma^+ + {}^3\Pi$. This KER is consistent with the ~6.4-eV KER of peak A_1.

As discussed earlier, peak A_2 may be due to above-threshold dissociation. One may also speculate that this higher-KER peak may be due to dissociation to the lowest dissociation limit ($^1\Sigma^+ + {}^1\Sigma^+$), but this requires significant spin-orbit coupling of the triplet and singlet states. A more complete theoretical treatment of the molecular structure and dissociation dynamics is needed to explore if this process is comparable to ATD. It is also important to recall that the $C_2D_2^{2+}$ ions in this study are vibrationally and rotationally hot, and therefore, the measured angular distributions do not give clear-cut guidance in determination of the dissociation pathways. Under these conditions, which may involve bending and asymmetric stretching, selection rules change because Λ (i.e., Σ, Π, Δ, ...) [57] is not a good quantum number and g/u symmetry does not apply.

The KER spectrum of the V channel, $C^+ + CD_2^+$, on the other hand, exhibits a single peak at ~7.4 eV, as shown in Fig. 5. Determining the dissociation pathways is more complex than the A-channel case and requires the complete potential energy surfaces on which the isomerization occurs. In this case, our measured KER is also significantly higher than the ~5-eV KER measured for this channel when probing a neutral C_2H_2 target with similar laser pulses [3]. Here again, the underlying reason for this difference is likely related to the different dynamics occurring in the triplet states, but detailed verification requires more complete structure calculations and better understanding of the strong-field isomerization process.

B. $C_2H_2^+$

For the $C_2H_2^+$ target, as previously reported [58], we observe both acetylene-like and vinylidene-like dissociation through the measurement of the $CH^+ + CH$ (A),
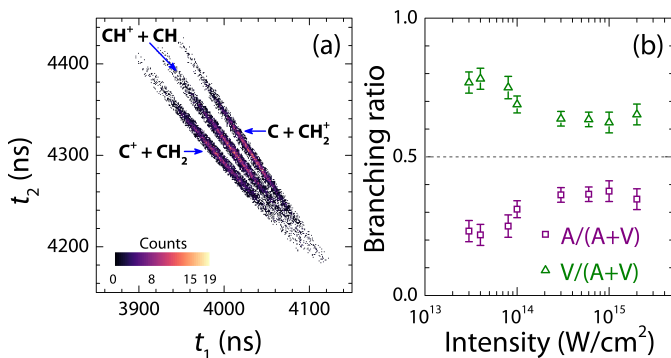
FIG. 6. (a) The CTOF spectrum of acetylene-like and vinylidene-like dissociation channels of a $C_2H_2^+$ target, measured with 790-nm pulses at a peak intensity of 6×10^{14} W/cm^2. (b) Laser intensity-dependent branching ratios of these dissociation channels. Note that $V = V_1 + V_2$.

$C^+ + CH_2$ (V_1), and $C + CH_2^+$ (V_2) channels, as highlighted in the CTOF spectrum in Fig. 6(a). Note that the presence of two vinylidene channels is due to the fact that either the C or CH$_2$ fragment can be positively charged. While this spectrum is zoomed in to focus on the dissociation channels of $C_2H_2^+$, we also measure the dissociative ionization channels $CH^+ + CH^+$ and $C^+ + CH_2^+$. For reference, at 6×10^{14} W/cm^2, the rate of the $CH^+ + CH^+$ channel is about half of that of the $CH^+ + CH$ channel. It is worth noting that the measured rate of the dissociative ionization channel $CH^+ + CH^+$ decreases relative to that of the dissociation channel $CH^+ + CH$ with decreasing intensity.

The intensity-dependent branching ratios for the dissociation channels are shown in Fig. 6(b), where the vinylidene channels are grouped ($V = V_1 + V_2$). The $\gtrsim 60\%$ vinylidene breakup branching ratio over all intensities suggests a significant amount of isomerization of the initial acetylene configuration $C_2H_2^+$ target. Also, the modulation of the branching ratio with laser intensity suggests some control over the isomerization process. Focal-volume averaging, which is important when ionization is not needed, likely reduces the observed intensity dependence.

The KER of the A and V dissociation channels, shown in Fig. 7(a)–(c), peak near 0 and die off approximately exponentially, extending up to ~3 eV. Exponential decay fits to these distributions are shown on the figures. Fast-decaying KER distributions peaking at low energies could indicate transitions to the vibrational continuum leading to dissociation upon a flat portion of a potential energy surface where little to no kinetic energy is gained [59]. The transition probability for such processes typically peaks near threshold and drops quickly with increasing energy above threshold [60]. The measured low KER of the A channel is consistent with the predicted flat surface towards dissociation for the ground state of the cation [61, 62]. This KER distribution of the A channel is also similar to results attributed to the breakup of $C_2H_2^+$

initiated by collisions of C_2H_2 with MeV projectiles [63].

Following assumptions similar to those in our discussion of $C_2D_2^{2+}$ dissociation pathways in Sec. III A, we first consider the case of $C_2H_2^+$ in its $X\,^2\Pi_u$ electronic ground state when probed by the laser. A few dissociation pathways starting from the $X\,^2\Pi_u$ state will yield the low KER that is measured for the $CH^+ + CH$ (A) channel. To discuss these possibilities, we turn to the potential energy curves of the linear acetylene monocation along the C–C stretch coordinate, reported by Perić and Engels (Fig. 7 in Ref. [62]). One candidate is a five-photon excitation from a low-lying vibrational level of the $X\,^2\Pi_u$ state to the $1\,^2\Pi_g$ state, followed by a C–C stretch and dissociation to the lowest $CH^+ + CH$ limit ($X\,^1\Sigma^+ + X\,^2\Pi$). Another possibility is a six-photon transition from a low-lying vibrational level of the $X\,^2\Pi_u$ state to the $1\,^2\Sigma_u^+$ state, leading to the first-excited $CH^+ + CH$ dissociation limit ($a\,^3\Pi + X\,^2\Pi$). Note that stimulated emission after some C–C stretch may lead to dissociation to the lowest $CH^+ + CH$ limit of the $X\,^2\Pi_u$ electronic ground state. Likewise, a seven-photon transition from the $X\,^2\Pi_u$ state to the $1\,^2\Sigma_g^+$ state (denoted as $A\,^2\Sigma_g^+$ in Refs. [12, 22, 24, 37]), followed by C–C stretching and stimulated emission to the electronic ground state will yield the measured KER. The latter pathway involves the $A\,^2\Sigma_g^+$ state invoked previously [12, 22, 24] to explain isomerization in the acetylene monocation.

The pathways described above include both parallel ($\Pi \leftrightarrow \Pi$) and perpendicular ($\Pi \leftrightarrow \Sigma$) transitions. The measured angular distributions should therefore include
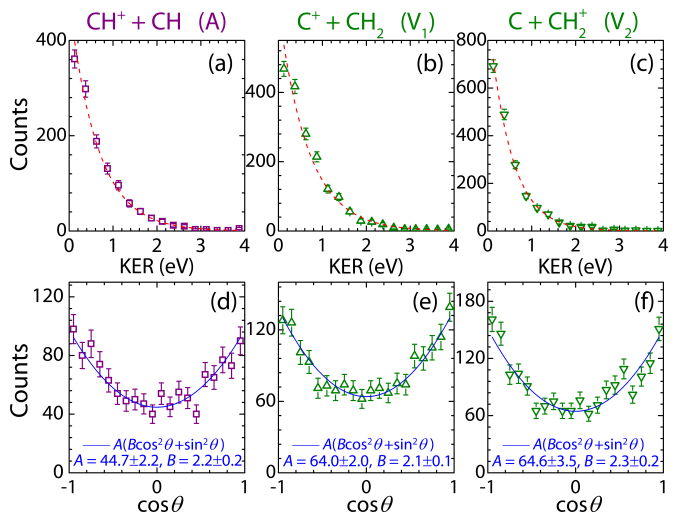
FIG. 7. The KER (top row) and angular (bottom row) distributions for the dissociation channels of $C_2H_2^+$ for laser pulses centered at 790 nm with peak intensity of 8×10^{13} W/cm^2. (a) and (d): $CH^+ + CH$. (b) and (e): $C^+ + CH_2$. (c) and (f): $C + CH_2^+$. The red dashed lines in (a)–(c) are exponential decay fits ($N_0\exp^{-KER/a}$) to the data. Note that θ is defined as the angle between the laser polarization and the momentum vector of the ionic fragment.

contributions peaking at both $\cos\theta = 0$ and ± 1 [60, 64, 65], as that in Fig. 7(d) does. This measured angular distribution, however, points to a lower photon number than the pathways mentioned above, which could mean that much higher lying vibrational levels of the $X\,{}^2\Pi_u$ state are involved instead.

The inquiry into plausible dissociation pathways becomes even richer upon consideration of the prediction by Hochlaf *et al.* [37] that the lowest quartet states of the acetylene cation, specifically the first-excited state, $1\,{}^4\Sigma_u^+$, and the lowest state, $1\,{}^4\Pi_g$, are long lived. The computed radiative lifetime of the $1\,{}^4\Sigma_u^+$ state [37] is much shorter than the flight time of the $C_2H_2^+$ molecules from the ion source to the interaction region (recall, $\sim 20\ \mu s$). Thus, $C_2H_2^+$ molecules in this state will decay to the lowest quartet state before reaching the interaction region. The lifetime of the $1\,{}^4\Pi_g$ state has not been reported, so it remains unclear if molecules in this state survive to be probed by the laser in our experiment.

For the sake of discussion, let us assume that the $1\,{}^4\Pi_g$ state does survive. The C–C stretch quartet potential energy curves calculated by Hochlaf *et al.* (Fig. 1(b) in Ref. [37]) suggest that highly-excited vibrational levels of the $1\,{}^4\Pi_g$ state would be populated, as this electronic state's minimum lies at a much larger C–C separation than that of neutral ground state C_2H_2. Thus, one-photon excitation from the $1\,{}^4\Pi_g$ state to the $1\,{}^4\Sigma_u^-$ or $1\,{}^4\Pi_u$ states can lead to $CH^+ + CH$ dissociation. These perpendicular and parallel transitions would also lead to angular distributions with contributions peaking at both $\cos\theta = 0$ and ± 1 but involving lower photon numbers than the proposed pathways involving doublet states. In this regard, the quartet pathways appear more consistent with the data presented in Fig. 7, hinting that the metastable state $1\,{}^4\Pi_g$ plays a key role. This possibility, however, awaits more careful investigation because it depends on the unknown lifetime of this quartet state.

Figures 7(e) and (f) show the angular distributions of the vinylidene channels, which are quite similar to the acetylene channel angular distribution. This similarity may indicate that the first excitation step is the same for all three channels, followed by propagation of the nuclear wave packet to different dissociation limits. Again, this speculation requires theoretical verification.

Identification of the pathways for vinylidene-like breakup requires information beyond what is readily available and thus calls for further work, which we hope our findings will encourage.

IV. SUMMARY AND OUTLOOK

In summary, we demonstrate a method to limit the isomerization dynamics of $C_2H_2^q$, a topic that has gen-

erated great interest, to a single charge state, avoiding the uncertainty caused by ionization. Even though the low density of an ion-beam target results in lower counting rates than those of gas-phase targets, as we have shown, we are still afforded the detailed array of information provided by coincidence 3D momentum imaging, including branching ratios, KER, and angular distributions. We have demonstrated use of this information to determine plausible dissociation pathways for acetylene-like breakup of the monocation and dication.

For excitation to a repulsive state, laser pulses of intensities lower than that needed for ionization may in principle be used, allowing one to reduce the contributions of complex multiphoton pathways. Alternatively, single-photon excitation [8, 66, 67] of these systems could also help in understanding the dynamics. The lack of ionization will also likely allow more direct comparisons with and guidance by theory. Thus, we anticipate that such an approach can facilitate a more thorough understanding of isomerization and fragmentation dynamics. While this manuscript leaves the door open in terms of reaching this deeper insight, we hope to have demonstrated our method to be one that has some advantages in molecular dynamics studies. We have also pointed out that many interesting avenues of study exist, such as control of the acetylene and vinylidene fragmentation branching ratios with different laser parameters.

Finally, on a more general note, one may readily recognize that this type of approach is not limited to exploring $C_2H_2^q$ isomerization. We anticipate that the use of molecular ion beams could be beneficial in examining bond rearrangement and other interesting strong-field dynamics in many different systems.

V. ACKNOWLEDGMENT

[1] T. Yatsuhashi and N. Nakashima, J. Photochem. Photobiol., C **34**, 52 (2018).

[2] T. Osipov, C. L. Cocke, M. H. Prior, A. Landers, T. Weber, O. Jagutzki, L. Schmidt, H. Schmidt-Böcking, and

R. Dörner, Phys. Rev. Lett. **90**, 233002 (2003).

[3] A. S. Alnaser, I. Litvinyuk, T. Osipov, B. Ulrich, A. Landers, E. Wells, C. M. Maharjan, P. Ranitovic, I. Bochareva, D. Ray, and C. L. Cocke, J. Phys. B **39**, S485 (2006).

[4] A. Hishikawa, A. Matsuda, M. Fushitani, and E. J. Takahashi, Phys. Rev. Lett. **99**, 258302 (2007).

[5] A. Hishikawa, A. Matsuda, E. J. Takahashi, and M. Fushitani, J. Chem. Phys. **128**, 084302 (2008).

[6] T. Osipov, T. N. Rescigno, T. Weber, S. Miyabe, T. Jahnke, A. S. Alnaser, M. P. Hertlein, O. Jagutzki, L. P. H. Schmidt, M. Schöffler, L. Foucar, S. Schössler, T. Havermeier, M. Odenweller, S. Voss, B. Feinberg, A. L. Landers, M. H. Prior, R. Dörner, C. L. Cocke, and A. Belkacem, J. Phys. B **41**, 091001 (2008).

[7] A. Matsuda, M. Fushitani, E. J. Takahashi, and A. Hishikawa, Phys. Chem. Chem. Phys. **13**, 8697 (2011).

[8] B. Gaire, S. Y. Lee, D. J. Haxton, P. M. Pelz, I. Bocharova, F. P. Sturm, N. Gehrken, M. Honig, M. Pitzer, D. Metz, H.-K. Kim, M. Schöffler, R. Dörner, H. Gassert, S. Zeller, J. Voigtsberger, W. Cao, M. Zohrabi, J. Williams, A. Gatton, D. Reedy, C. Nook, T. Müller, A. L. Landers, C. L. Cocke, I. Ben-Itzhak, T. Jahnke, A. Belkacem, and T. Weber, Phys. Rev. A **89**, 013403 (2014).

[9] X. Gong, Q. Song, Q. Ji, H. Pan, J. Ding, J. Wu, and H. Zeng, Phys. Rev. Lett. **112**, 243001 (2014).

[10] X. Xie, K. Doblhoff-Dier, H. Xu, S. Roither, M. S. Schöffler, D. Kartashov, S. Erattupuzha, T. Rathje, G. G. Paulus, K. Yamanouchi, A. Baltuška, S. Gräfe, and M. Kitzler, Phys. Rev. Lett. **112**, 163003 (2014).

[11] C. E. Liekhus-Schmaltz, I. Tenney, T. Osipov, A. Sanchez-Gonzalez, N. Berrah, R. Boll, C. Bomme, C. Bostedt, J. D. Bozek, S. Carron, R. Coffee, J. Devin, B. Erk, K. R. Ferguson, R. W. Field, L. Foucar, L. J. Frasinski, J. M. Glownia, M. Gühr, A. Kamalov, J. Krzywinski, H. Li, J. P. Marangos, T. J. Martinez, B. K. McFarland, S. Miyabe, B. Murphy, A. Natan, D. Rolles, A. Rudenko, M. Siano, E. R. Simpson, L. Spector, M. Swiggers, D. Walke, S. Wang, T. Weber, P. H. Bucksbaum, and V. S. Petrovic, Nat. Commun. **6**, 8199 (2015).

[12] X. Gong, Q. Song, Q. Ji, K. Lin, H. Pan, J. Ding, H. Zeng, and J. Wu, Phys. Rev. Lett. **114**, 163001 (2015).

[13] M. Kübel, R. Siemering, C. Burger, N. G. Kling, H. Li, A. S. Alnaser, B. Bergues, S. Zherebtsov, A. M. Azzeer, I. Ben-Itzhak, R. Moshammer, R. de Vivie-Riedle, and M. F. Kling, Phys. Rev. Lett. **116**, 193001 (2016).

[14] C. Burger, N. G. Kling, R. Siemering, A. S. Alnaser, B. Bergues, A. M. Azzeer, R. Moshammer, R. de Vivie-Riedle, M. Kübel, and M. F. Kling, Faraday Discuss. **194**, 495 (2016).

[15] M. Kübel, C. Burger, R. Siemering, N. G. Kling, B. Bergues, A. S. Alnaser, I. Ben-Itzhak, R. Moshammer, R. de Vivie-Riedle, and M. F. Kling, Mol. Phys. **115**, 1835 (2017).

[16] Z. Li, L. Inhester, C. Liekhus-Schmaltz, B. F. E. Curchod, J. W. Snyder, N. Medvedev, J. Cryan, T. Osipov, S. Pabst, O. Vendrell, P. Bucksbaum, and T. J. Martinez, Nat. Commun. **8**, 453 (2017).

[17] C. Burger, A. Atia-Tul-Noor, T. Schnappinger, H. Xu, P. Rosenberger, N. Haram, S. Beaulieu, F. Légaré, A. S. Alnaser, R. Moshammer, R. T. Sang, B. Bergues, M. S. Schuurman, R. de Vivie-Riedle, I. V. Litvinyuk, and

[18] M. F. Kling, Struct. Dyn. **5**, 044302 (2018).

[18] R. Dörner, V. Mergel, O. Jagutzki, L. Spielberger, J. Ullrich, R. Moshammer, and H. Schmidt-Böcking, Phys. Rep. **330**, 95 (2000).

[19] J. Ullrich, R. Moshammer, A. Dorn, R. Dörner, L. P. H. Schmidt, and H. Schmidt-Böcking, Rep. Prog. Phys. **66**, 1463 (2003).

[20] A. M. Sayler, E. Eckner, J. McKenna, B. D. Esry, K. D. Carnes, I. Ben-Itzhak, and G. G. Paulus, Phys. Rev. A **97**, 033412 (2018).

[21] I. Luzon, E. Livshits, K. Gope, R. Baer, and D. Strasser, J. Phys. Chem. Lett. **10**, 1361 (2019).

[22] Y. H. Jiang, A. Rudenko, O. Herrwerth, L. Foucar, M. Kurka, K. U. Kühnel, M. Lezius, M. F. Kling, J. van Tilborg, A. Belkacem, K. Ueda, S. Düsterer, R. Treusch, C. D. Schröter, R. Moshammer, and J. Ullrich, Phys. Rev. Lett. **105**, 263002 (2010).

[23] Y. H. Jiang, A. Senftleben, M. Kurka, A. Rudenko, L. Foucar, O. Herrwerth, M. F. Kling, M. Lezius, J. V. Tilborg, A. Belkacem, K. Ueda, D. Rolles, R. Treusch, Y. Z. Zhang, Y. F. Liu, C. D. Schrter, J. Ullrich, and R. Moshammer, J. Phys. B **46**, 164027 (2013).

[24] H. Ibrahim, B. Wales, S. Beaulieu, B. E. Schmidt, N. Thiré, E. P. Fowe, E. Bisson, C. T. Hebeisen, V. Wanie, M. Giguére, J.-C. Kieffer, M. Spanner, A. D. Bandrauk, J. Sanderson, M. S. Schuurman, and F. Légaré, Nat. Commun. **5**, 4422 (2014).

[25] J. H. D. Eland, F. S. Wort, P. Lablanquie, and I. Nenner, Z. Phys. D: At., Mol. Clusters **4**, 31 (1986).

[26] E. Wells, C. Rallis, M. Zohrabi, R. Siemering, B. Jochim, P. Andrews, U. Ablikim, B. Gaire, S. De, K. Carnes, B. Bergues, R. de Vivie-Riedle, M. Kling, and I. Ben-Itzhak, Nat. Commun. **4**, 2895 (2013).

[27] S.-H. Zheng and S. K. Srivastava, J. Phys. B **29**, 3235 (1996).

[28] G. Josifov, D. Lukic, N. Uric, and M. Kurepa, J. Serb. Chem. Soc. **65**, 517 (2000).

[29] S. Feil, K. Głuch, A. Bacher, S. Matt-Leubner, D. K. Böhme, P. Scheier, and T. D. Märk, J. Chem. Phys. **124**, 214307 (2006).

[30] S. Feil, P. Sulzer, A. Mauracher, M. Beikircher, N. Wendt, A. Aleem, S. Denifl, F. Zappa, S. Matt-Leubner, A. Bacher, S. Matejcik, M. Probst, P. Scheier, and T. D. Märk, J. Phys.: Conf. Ser. **86**, 012003 (2007).

[31] Acetylene is a common product of methane in plasma environments through the recombination of CH_x radicals [68–72].

[32] H. Helm and P. C. Cosby, J. Chem. Phys. **86**, 6813 (1987).

[33] Z. Amitay, A. Baer, M. Dahan, J. Levin, Z. Vager, D. Zajfman, L. Knoll, M. Lange, D. Schwalm, R. Wester, A. Wolf, I. F. Schneider, and A. Suzor-Weiner, Phys. Rev. A **60**, 3769 (1999).

[34] F. von Busch and G. H. Dunn, Phys. Rev. A **5**, 1726 (1972).

[35] A. M. Sayler, P. Q. Wang, K. D. Carnes, and I. Ben-Itzhak, J. Phys. B **40**, 4367 (2007).

[36] M. Zohrabi, J. McKenna, B. Gaire, N. G. Johnson, K. D. Carnes, S. De, I. A. Bocharova, M. Magrakvelidze, D. Ray, I. V. Litvinyuk, C. L. Cocke, and I. Ben-Itzhak, Phys. Rev. A **83**, 053405 (2011).

[37] M. Hochlaf, S. Taylor, and J. H. D. Eland, J. Chem. Phys. **125**, 214301 (2006).

[38] X. Ren, A. M. Summers, Kanaka Raju P., A. Vajdi, V. Makhija, C. W. Fehrenbach, N. G. Kling, K. J. Betsch, Z. Wang, M. F. Kling, K. D. Carnes, I. Ben-Itzhak, C. Trallero-Herrero, and V. Kumarappan, J. Opt. **19**, 124017 (2017).

[39] R. Trebino, K. W. DeLong, D. N. Fittinghoff, J. N. Sweetser, M. A. Krumbgel, B. A. Richman, and D. J. Kane, Rev. Sci. Instrum. **68**, 3277 (1997).

[40] P. Wang, A. M. Sayler, K. D. Carnes, B. D. Esry, and I. Ben-Itzhak, Opt. Lett. **30**, 664 (2005).

[41] R. W. Boyd, *Nonlinear Optics, Third Edition*, 3rd ed. (Academic Press, Inc., Orlando, FL, USA, 2008).

[42] D. J. Kane and R. Trebino, IEEE J. Quantum Electron. **29**, 571 (1993).

[43] I. Ben-Itzhak, P. Q. Wang, J. F. Xia, A. M. Sayler, M. A. Smith, K. D. Carnes, and B. D. Esry, Phys. Rev. Lett. **95**, 073002 (2005).

[44] P. Q. Wang, A. M. Sayler, K. D. Carnes, J. F. Xia, M. A. Smith, B. D. Esry, and I. Ben-Itzhak, Phys. Rev. A **74**, 043411 (2006).

[45] A. M. Sayler, *Measurements of Ultrashort Intense Laser-Induced Fragmentation of Simple Molecular Ions*, Ph.D. thesis, Kansas State University (2008).

[46] B. Gaire, *Imaging of slow dissociation of the laser induced fragmentation of molecular Ions*, Ph.D. thesis (2011).

[47] B. Gaire, J. McKenna, M. Zohrabi, K. D. Carnes, B. D. Esry, and I. Ben-Itzhak, Phys. Rev. A **85**, 023419 (2012).

[48] S. Kaziannis, N. Kotsina, and C. Kosmidis, J. Chem. Phys. **141**, 104319 (2014).

[49] H. Li, N. G. Kling, B. Frg, J. Stierle, A. Kessel, S. A. Trushin, M. F. Kling, and S. Kaziannis, Struct. Dyn. **3**, 043206 (2016).

[50] Atia-tul-noor, N. Haram, H. Xu, U. S. Sainadh, R. T. Sang, and I. V. Litvinyuk, Phys. Rev. A **97**, 033402 (2018).

[51] X. Xie, K. Doblhoff-Dier, S. Roither, M. S. Schöffler, D. Kartashov, H. Xu, T. Rathje, G. G. Paulus, A. Baltuška, S. Gräfe, and M. Kitzler, Phys. Rev. Lett. **109**, 243001 (2012).

[52] X. Xie, S. Roither, M. Schöffler, E. Lötstedt, D. Kartashov, L. Zhang, G. G. Paulus, A. Iwasaki, A. Baltuška, K. Yamanouchi, and M. Kitzler, Phys. Rev. X **4**, 021005 (2014).

[53] X. Xie, E. Lötstedt, S. Roither, M. Schöffler, D. Kartashov, K. Midorikawa, A. Baltuška, K. Yamanouchi, and M. Kitzler, Sci. Rep. **5**, 12877 (2015).

[54] Q. Song, X. Gong, Q. Ji, K. Lin, H. Pan, J. Ding, H. Zeng, and J. Wu, J. Phys. B **48**, 094007 (2015).

[55] H. Li, N. G. Kling, T. Gaumnitz, C. Burger, R. Siemering, J. Schötz, Q. Liu, L. Ban, Y. Pertot, J. Wu, A. M. Azzeer, R. de Vivie-Riedle, H. J. Wörner, and M. F. Kling, Opt. Express **25**, 14192 (2017).

[56] R. Thissen, J. Delwiche, J. M. Robbe, D. Duflot, J. P. Flament, and J. H. D. Eland, J. Chem. Phys. **99**, 6590 (1993).

[57] Λ is the projection of the total electron orbital angular momentum on the molecular axis of linear HCCH.

[58] B. Jochim, B. Berry, T. Severt, P. Feizollah, M. Zohrabi, Kanaka Raju P., E. Wells, K. D. Carnes, and I. Ben-Itzhak, J. Phys. Chem. Lett. **10**, 2320 (2019).

[59] W. Demtröder, *Atoms, Molecules and Photons: an introduction to Atomic-, Molecular- and Quantum physics* (Springer, 2018).

[60] A. M. Sayler, P. Q. Wang, K. D. Carnes, B. D. Esry, and I. Ben-Itzhak, Phys. Rev. A **75**, 063420 (2007).

[61] M. Davister and R. Locht, Chem. Phys. **191**, 333 (1995).

[62] M. Perić and B. Engels, Chem. Phys. **238**, 47 (1998).

[63] S. Yoshida, T. Majima, T. Asai, M. Matsubara, H. Tsuchida, M. Saito, and A. Itoh, Nucl. Instrum. Methods Phys. Res., Sect. B **408**, 203 (2017), proceedings of the 18th International Conference on the Physics of Highly Charged Ions (HCI-2016), Kielce, Poland, 11-16 September 2016.

[64] R. N. Zare, Mol. Photochem. **4**, 1 (1972).

[65] A. Hishikawa, S. Liu, A. Iwasaki, and K. Yamanouchi, J. Chem. Phys. **114**, 9856 (2001).

[66] P. C. Cosby, R. Möller, and H. Helm, Phys. Rev. A **28**, 766 (1983).

[67] H. B. Pedersen, S. Altevogt, B. Jordon-Thaden, O. Heber, M. L. Rappaport, D. Schwalm, J. Ullrich, D. Zajfman, R. Treusch, N. Guerassimova, M. Martins, J.-T. Hoeft, M. Wellhöfer, and A. Wolf, Phys. Rev. Lett. **98**, 223202 (2007).

[68] M. Ioffe, S. Pollington, and J. Wan, J. Catal. **151**, 349 (1995).

[69] A. V. Kirikov, V. V. Ryzhov, and A. I. Suslov, Tech. Phys. Lett. **25**, 794 (1999).

[70] M. Heintze, M. Magureanu, and M. Kettlitz, J. Appl. Phys. **92**, 7022 (2002).

[71] G.-B. Zhao, S. John, J.-J. Zhang, L. Wang, S. Muknahallipatna, J. C. Hamann, J. F. Ackerman, M. D. Argyle, and O. A. Plumb, Chem. Eng. J. **125**, 67 (2006).

[72] C. Shen, Y. Sun, D. Sun, and H. Yang, Sci. China: Chem. **53**, 231 (2010).